

ON THE MODELLING AND THE PREDICTION OF THE VIBROACOUSTIC BEHAVIOUR OF AN AIRCRAFT STRUCTURE

Li Cheng* and Jean Nicolas

G.A.U.S., Mechanical Engineering Department, University of Sherbrooke, Québec, J1K 2R1 Canada

ABSTRACT

This paper summarizes the first step of a long-term research program focusing on the modeling and prediction of the vibrational and acoustical behavior of an aircraft structure. The final goal pursued is to provide the aeronautical industry with guidance for cabin sound-proofing with the help of a versatile, physical and easy-to-use model. Two main subjects tackled in this paper are: ① The free vibrational behavior of the aircraft structure. ② Effects of the rear pressure bulkhead on the cabin noise.

SOMMAIRE

Ce papier résume la première étape d'une série de programme de recherche portant sur la modélisation et la prédiction du comportement vibratoire et acoustique de structure d'avion. L'objectif final est de fournir à l'industrie aéronautique, à l'aide d'un modèle qui est à la fois physique et propice à l'analyse paramétrique, des directives en vue de l'amélioration de la discrétion acoustique dans la cabine. Deux sujets principaux traités sont les suivants: ① Comportement de vibration libre de la structure d'avion. ② Effets de la cloison arrière sur le bruit interne de la cabine.

1. INTRODUCTION

Noise inside the aircraft cabin affects passenger speech communication, comfort, composure and sleep. Consequently, control of interior noise is required as one of the key elements in enhancing the competitiveness of new-generation aircraft in the commercial markets. Unremitting efforts to increase aircraft performance and to reduce weight and fuel consumption present new challenges for noise control technology. To meet these challenges, substantial research and development have been carried out. But much research is still needed in this field. In this paper, we present some preliminary results regarding the modeling and the prediction of the vibrational and acoustical behavior of an aircraft structure.

1.1 Noise sources

It is beyond the scope of this paper to review all of the past theoretical and experimental work on interior noise. Readers are referred to references [1-2] for classical work and [3] for more recent development in the field. It is generally

(*) This paper reports the research activities carried out by the first author during his tenure as the first holder of the CAA Edgar and Millicent Shaw Postdoctoral Prize in Acoustics, 1990 and 1991.

(*) Current address: Mechanical Engineering Department, Université Laval, Québec, G1K 7P4 Canada

admitted that aircraft noise prediction and control are very complex subjects. First of all, the noise sources have to be identified before a representative model is established. Usually, cabin noise sources include propellers, exhaust from reciprocating or turbofan engines, turbomachinery, turbulent flow over the aircraft structure and engine vibrations [3]. Noise from internal sources, such as air-conditioning systems, may also be important in some situations. Secondly, noise transmission involves very complicated mechanisms, whose understanding is indispensable to the choice of any noise control measures. Generally speaking, noise is transmitted to the cabin along airborne paths through the fuselage sidewall and along structure borne paths, through mechanical connections such as engine mounts. In both cases, structural vibration and the acoustical field inside the cabin form a complicated coupled system. The coupling process is illustrated schematically in Fig. 1. It shows clearly that three physical mechanisms (structural vibration, radiation and fluid-structure interaction) have to be accounted for jointly. This statement is also confirmed by a common observation, which may appear striking to those who are not familiar with the problems: the decrease in vibration level can not always guarantee the same trend for sound levels. Therefore, a throughout understanding of the "why" and the "how" of this fluid-structure interaction is fundamental.

1.2 Simulation models

Faced with such problems, several approaches are available. The first involves numerical procedures, such as Finite Element Method (FEM) and Boundary Element Method (BEM) [4]. A particular advantage of these methods is that they can deal with mathematical models representing very detailed idealizations of the physical structures. However, they depend heavily on large, fast computational facilities. The computational demands increase dramatically with the structural size and frequency range of interest. Even today, when computational methods are highly developed and optimized, it is only practicable to predict the aircraft's behavior at very low frequencies[5]. Most importantly, the methods do not allow easy parametric studies and offer little physical insight into the physical phenomena. Another applicable method is referred to as Statistical Energy Analysis (SEA)[6]. This method involves a lot of hypotheses and gives only rough estimates in relatively broad frequency bands at higher frequencies. Up to now, it is still not a predictive method since some of the important parameters must be obtained by experiment[7]. The third category involves analytical methods for the simple reason that discretization is not applied to the governing equations, as in the case of FEM, but to the solutions at a later stage. This method overcomes the shortcomings of the two forementioned methods, though the method is up to now applicable only to structures of simple geometry. The philosophy of using this method is to reveal the main physical processes without considering the details of the structures. This is believed, in some circumstances, to be sufficient to guide noise control actions.

1.3 New models

In this paper, we present a new model for airplane cabin noise prediction. This model is based essentially on the work done by Cheng *et al.*; detailed development of the model is given in references [8-9]. The approach can be classified as an analytical one, but further development is made to extend the existing models to a more general context in order to address more complicated fuselage structure. The study is part of a program of work undertaken on an aircraft "Challenger 601-3A" (Canadair) by the authors in order to investigate the noise and vibration produced by the engines. Preliminary testing on real aircraft has identified significant sources of mechanical excitation transmitted from the engines. The engines are attached directly to the aircraft body through beams in the rear part where a Rear Pressure Bulkhead (RPB) is fixed (Fig.2). Therefore, the aircraft fuselage and the RPB are considered as the main components affecting the cabin noise. In the light of these observations, a model, consisting of a circular cylindrical shell and an end panel is used to simulate the aircraft structure. Elastic coupling is permitted between these two substructures. This point, together with the consideration of the end plate, constitutes a novel element with respect to existing models in the

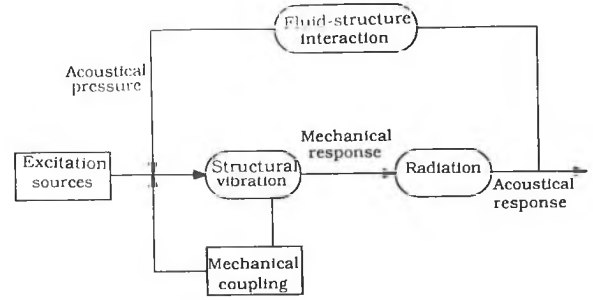


Fig.1 Schematic diagram of the coupling process

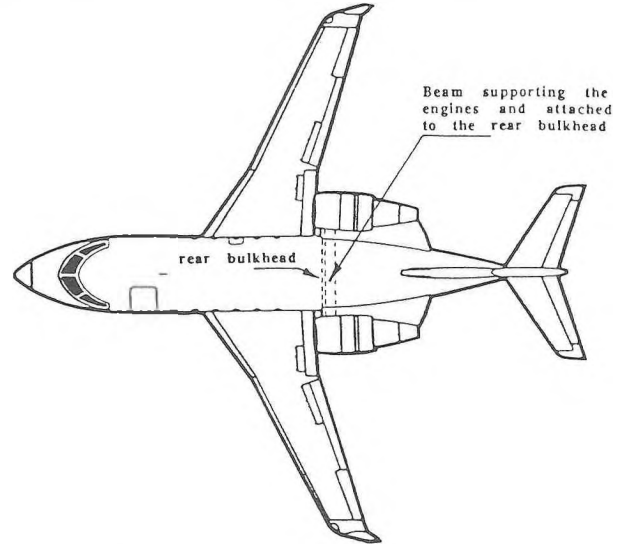


Fig.2. Schematic drawing of the airplane and the location of the Rear Pressure Bulkhead

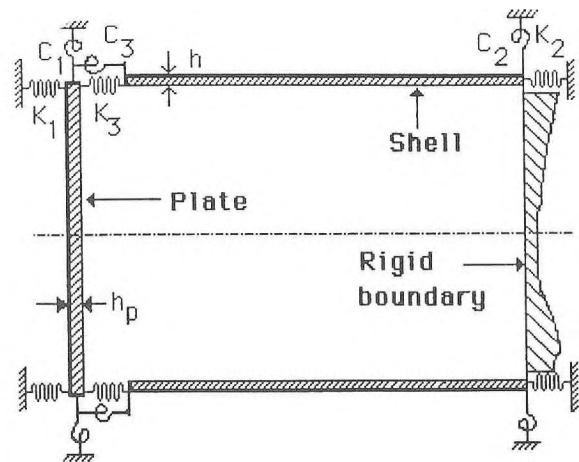


Fig.3. Model investigated

literature [10-12]. It permits varying the type of junction from free to rigid. Starting with a brief review of the formulation, we outline the basic steps. The paper is not intended to make a lengthy presentation of the formulation;

instead, emphasis is placed on phenomenal interpretations. First, numerical results are presented and interpreted in terms of the free vibration of the structure, illustrating the main coupling phenomena between the shell and the plate. Comparisons are also made with finite element analysis to show the convenience, efficiency and accuracy of our model. Second, emphasis is placed on the fixing condition of the Rear Pressure Bulkhead to the fuselage. This section ends with some discussion of the possibility of sound-proofing by choosing appropriately the fixation of the RPB.

2. MODEL INVESTIGATED

Fig. 3 shows the cross section of the model investigated. It consists of a finite, circular, thin, cylindrical shell with a circular plate at the left end. An acoustically rigid wall (with infinite impedance) is placed at the right end of the structure to form an acoustic cabin. The origin of the coordinate system is set at the geometrical center of the plate and, consequently, each point of the structure is located by x, q, r which correspond respectively to the longitudinal, tangential and radial directions. u, v and w are the displacements of the shell along these three directions. The shell is initially assumed to be supported by shear diaphragms at each end so that the v and w components are restrained at the boundary. For the plate, only the normal displacement w_p of the plate is taken into account and it is assumed positive along the positive x -axis. The plate has a thickness h_p and is elastically supported by translational springs and rotational springs having, respectively, distributed stiffness K_1 (N/m^2) and C_1 (Nm/m) along its edge. Similar spring systems are introduced between the plate and the shell (K_3, C_3) and at the right end of the shell (K_2, C_2). All the spring constants are defined in the appropriate units of stiffness per unit length on the contour and are assumed to be constant along the edges. Point forces may be applied to the structure. In what follows, the sound field within the cavity, as well as the vibration of the structure, will be calculated. The effect of the fluid loading from the outside of the cavity on the structure's vibration will be neglected.

3. THEORY

3.1 Basic Equations:

Structural vibration:

$$dH = 0 \quad (1)$$

$$H = \int_0^{t_1} (T_c - E_c + T_p - E_p - E_k - E_f) dt \quad (2)$$

where T_c and T_p are, respectively, the kinetic energies of the cylindrical shell and the plate, E_c and E_p are their potential energies, E_k represents the potential energy stored in the springs, and E_f the work done by external driving forces and by internal acoustic pressure.

Acoustical field:

$$\nabla^2 P_c + (\omega/c)^2 P_c = 0 \quad (3)$$

in which P_c is the sound pressure inside the cavity, ω is the excitation angular frequency and c is speed of sound.

Fluid-structure interface condition:

$$\begin{cases} \frac{\partial P_c}{\partial \xi} = \rho \omega^2 w_p & \text{on } A_p \\ \frac{\partial P_c}{\partial \xi} = -\rho \omega^2 w & \text{on } A_c \\ \frac{\partial P_c}{\partial \xi} = 0 & \text{on } A_R \end{cases} \quad (4)$$

where ρ is the fluid density, A_c and A_p are, respectively, the surface of the shell and the plate, A_R is the rigid portion of the cavity wall surface, and ξ is the unit normal to the corresponding surface (positive towards the outside).

Remarks:

- 1) Eq. (1) is the mathematical expression of the well known Hamilton's principle, which states that the displacement of a system adjusts itself in shape and velocity so that the Hamilton's function H is minimized.
- 2). Eq. (3) is the classical Helmholtz equation that governs the acoustical field inside the cavity.
- 3). Structure-cavity coupling in the system is characterized by the term E_f in Eq. (2) and by the fluid-structure interface condition.

3.2 Solution Discretization and Coupling Equations

Solution discretization

The whole set of equations given above can be resolved by discretizing different unknowns on the basis of appropriately chosen series. The appropriate choice of these series is a crucial factor on which the accuracy of the prediction depends. This is not an easy task, especially when the structure is complex and when different movements are involved. The difficulty is also increased by

the fact that unsuitable choices may make numerical treatment very lengthy and heavy.

For the shell:

The eigenfunctions of the "shear-diaphragm-supported" shell are used as admissible functions and expansion of the displacement components is expressed as:

$$\begin{Bmatrix} u \\ v \\ w \end{Bmatrix} = \sum_{\alpha=0}^1 \sum_{n=0}^{\infty} \sum_{m=1}^{\infty} \sum_{j=1}^3 A_{nmj}^{\alpha}(t) \Gamma_{nmj}^{\alpha}$$

$$\Gamma_{nmj}^{\alpha} = \begin{Bmatrix} D_{nmj} \sin(n\theta + \alpha\pi/2) \cos(m\pi x/L) \\ E_{nmj} \cos(n\theta + \alpha\pi/2) \sin(m\pi x/L) \\ \sin(n\theta + \alpha\pi/2) \sin(m\pi x/L) \end{Bmatrix} \quad (5)$$

where $(D_{nmj}, E_{nmj}, 1)$ are the components of the eigenvector; n and m are, respectively, the circumferential and longitudinal order; α denotes symmetric ($\alpha=1$) or antisymmetric ($\alpha=0$) modes and j denotes the type of modes (bending, twisting, extension-compression).

$A_{nmj}^{\alpha}(t)$ are the coefficients to be determined.

For the plate:

The expansion of the plate's displacement is expressed as:

$$w_p(t) = \sum_{\alpha=0}^1 \sum_{n=0}^{\infty} \sum_{m_p=0}^{\infty} B_{nm_p}^{\alpha}(t) \Lambda_{nm_p}^{\alpha}$$

$$\Lambda_{nm_p}^{\alpha} = \sin(n\theta + \alpha\pi/2) \left(\frac{r}{a}\right)^{m_p} \quad (6)$$

with n, m_p and α being, respectively, the circumferential

order, the radial order and the symmetry index. $B_{nm_p}^{\alpha}(t)$ are coefficients to be determined.

For the cavity:

For the cylindrical cavity considered here, the normal modes for the case of acoustically hard walls are known analytically. The pressure inside the cavity can thus be expanded in terms of these cavity modes as:

$$P_c = \sum_{\alpha=0}^1 \sum_{n=0}^{\infty} \sum_{p=1}^{\infty} \sum_{q=1}^{\infty} P_{npq}^{\alpha}(t) \Phi_{npq}^{\alpha}$$

$$\Phi_{npq}^{\alpha} = \sin\left(n\theta + \alpha\frac{\pi}{2}\right) J_n(\lambda_{np} r) \cos\left(\frac{q\pi}{L} x\right) \quad (7)$$

where α is the symmetry index, n is the circumferential order, J_n is the n th order Bessel function, q is the longitudinal order and λ_{np} is the p th root of the following equation:

$$J_n'(\lambda_{np} a) = 0 \quad (8)$$

Coupling equations

For structure vibration:

Using expressions (5) and (6) to calculate different energy terms involved in Eq. (2), one expresses the Hamilton's

function H in terms of two sets of unknowns, $A_{nmj}^{\alpha}(t)$

and $B_{nm_p}^{\alpha}(t)$.

The minimization of H with respect to these unknowns according to Lagrange equation yields a set of ordinary differential equations. It should be noted at this stage that these structural unknowns are coupled to the acoustical pressure P_c , whose determination, in turn, depends on the structural vibration.

For acoustic field:

The sound pressure P_c inside the cavity can be calculated by means of the cavity Green's function G with Neumann boundary conditions [9] as follows:

$$P_c = - \int_{A_p} G \rho \omega^2 w_p dA_p + \int_{A_c} G \rho \omega^2 w dA_c \quad (9)$$

The Green's function G in the cylindrical cavity is known analytically. It is expressed in the form of cavity mode decomposition.

Inserting Eq. (7) into (9) yields another set of ordinary differential equations describing the interior sound pressure.

Coupling equations:

The equations obtained above may be summarized schematically as follows:

$$\left[S \right] \begin{Bmatrix} A_{nmj}^{\alpha} \\ B_{nm_p}^{\alpha} \\ P_{npq}^{\alpha} \end{Bmatrix} = \begin{Bmatrix} F_{nmj}^{\alpha(\text{shell})} \\ \alpha(\text{plate}) \\ F_{nm_p}^{\alpha} \\ 0 \end{Bmatrix} \quad (10)$$

in which matrix S is the system matrix. The three sets of unknowns are related, respectively, to the shell, plate vibration and cavity sound pressures. The three terms of the right hand side are generalized forces corresponding to the decomposition terms of the shell and the plate.

Remarks:

- 1) The system should be resolved as a whole.
- 2) Two types of problem can be solved by using the established model: free vibrational analysis of the structure in vacuum, and structure-cavity coupling. The free vibrational study of the structure is done by neglecting the terms in the system (10) corresponding to the excitation and cavity. The solution of this eigenvalue equation yields the natural frequencies together with the coefficients for constituting the mode shapes. The structure-cavity coupling analysis, is done by solving system(10). Two main parameters which will be used in the analysis are the average quadratic velocity $\langle v^2 \rangle$ of the structure and the average sound pressure level L_p inside the cavity.
- 3) The size of the system depends on the truncation of the series (5),(6), and (7). For the structure, the number of terms used in the series is increased until a relatively stable solution is achieved. It has been observed during numerical calculations that the solution converges rather rapidly for free vibration problems. For response prediction, the decomposition term is increased until all resonance modes in the frequency range of interest are reasonably well predicted. As far as the cavity is concerned, all cavity modes whose natural frequencies are included in the frequency band considered have been taken in the expansion (7) for each calculation.

4. RESULTS AND DISCUSSION

4.1 Free vibration of the structure

The versatility of this model has been demonstrated in the previous work [8]. In fact, this model can be used to investigate the vibrational behavior of a single plate, a single shell or their combination. The characterization of structural coupling and boundary conditions by means of continuous distributions of springs along the shell and the plate interface allows a wide spectrum of boundary conditions and coupling conditions between the shell and the plate. In that paper, very good precision of the method has been demonstrated by solving test problems for lower-order modes of the plate and the shell for which some results are available in the literature. Here, we perform a supplementary comparison with Finite Element Analysis of a plate-ended shell. The objective is to compare two methods with respect to precision and CPU time, and to illustrate the physical process by which two sub-structures are coupled.

The shell and plate considered are assumed to have the same thicknesses and material properties. The geometrical parameters used are $a/h = 30$, $L/a = 3$ (a being the radius, h the thickness and L the length). The shell is "shear diaphragm supported" at the right end ($X = L$) and rigidly connected to the plate at the left end ($X = 0$). With this structure, the lower-order modes are calculated by both methods and the comparisons are made in terms of frequency parameters, CPU time, memory space required and mode shapes. The so-called frequency parameter Ω , which is a dimensionless quantity, is the ratio between the natural frequency and the ring frequency, the latter being defined as:

$$f_r = 1 / (2\pi a) \sqrt{E / \rho_s (1 - \nu^2)} \quad (11)$$

where E and ρ_s are, respectively, the Young's modulus and the density of the material.

The finite element software used is available commercially (ANSYS 4.4A). A 19 x 20 finite element mesh (in the circumferential and longitudinal directions respectively) is used for the shell and a 20 x 20 mesh (in the circumferential and radial directions respectively) for the plate. This meshing is illustrated in Fig.4. All calculations are carried out with the computer IRIS-4D.

The frequency parameters are compared in Table I. It can be seen that the two sets of results agree within 5% and that most of modes are predicted with a better precision. As far as CPU time is concerned, our method is far more rapid than FEM. It should be noted that our calculation was carried out for every given circumferential order n and each calculation was completed within 20.6 second. This calculation speed will be the same even if the higher order n is pursued. As for FEM, the CPU time and memory space required increase dramatically with n , for the simple reason that more finite elements are needed at that time.

Figure 4 compares the first three modes shapes for $n = 2$ calculated by our model and by FEM. The three pictures in the left column are the results given by our calculation. These figures show the normal displacement of the plate (w_p) and the radial displacement of the shell (w) in the cross section with $\theta = 0$ and $\theta = \pi$. Pictures in the next two columns are FEM results for the same modes. Two observations can be made: 1). The agreement between the two sets of results is excellent. The two approaches give exactly the same description of the structural motion and even the very detailed deformation around the shell-plate junction is precisely predicted. 2). These pictures show the two types of modes of the combined structure: the first is dominated by shell vibration; the second is essentially a plate mode. The third possible type is a well-coupled mode,

Table I. Comparison of frequency parameters between the present study and Finite Element Method in the case of a plate-ended shell ($L/a = 3$, $a/h = 30$)^{*}

Mode n	Order q	Our study	FEM	Deviation ξ in %
3	1	0.1566	0.15026	4.0%
4	1	0.1728	0.1738	0.58%
1	1	0.1866	0.1801	3.4%
2	1	0.2258	0.2201	2.5%
5	1	0.2443	0.2499	-2.2%
4	2	0.2856	0.2861	0.2%
2	2	0.3078	0.3028	1.6%
5	2	0.3128	0.3142	-0.4%
3	2	0.3344	0.3350	-0.18%
1	2	0.3998	0.3813	4.6%
3	3	0.4480	0.4433	1.0%
4	3	0.4338	0.4415	-1.8%
2	3	0.4742	0.4745	-0.07%
1	3	0.5579	0.5224	2.8%
CPU time		103 sec.	5751 sec.	ratio: 56
Mem. space		2 meg	20 meg	ratio: 10

* q : mode rank
 ξ : (present study-FEM)/present study

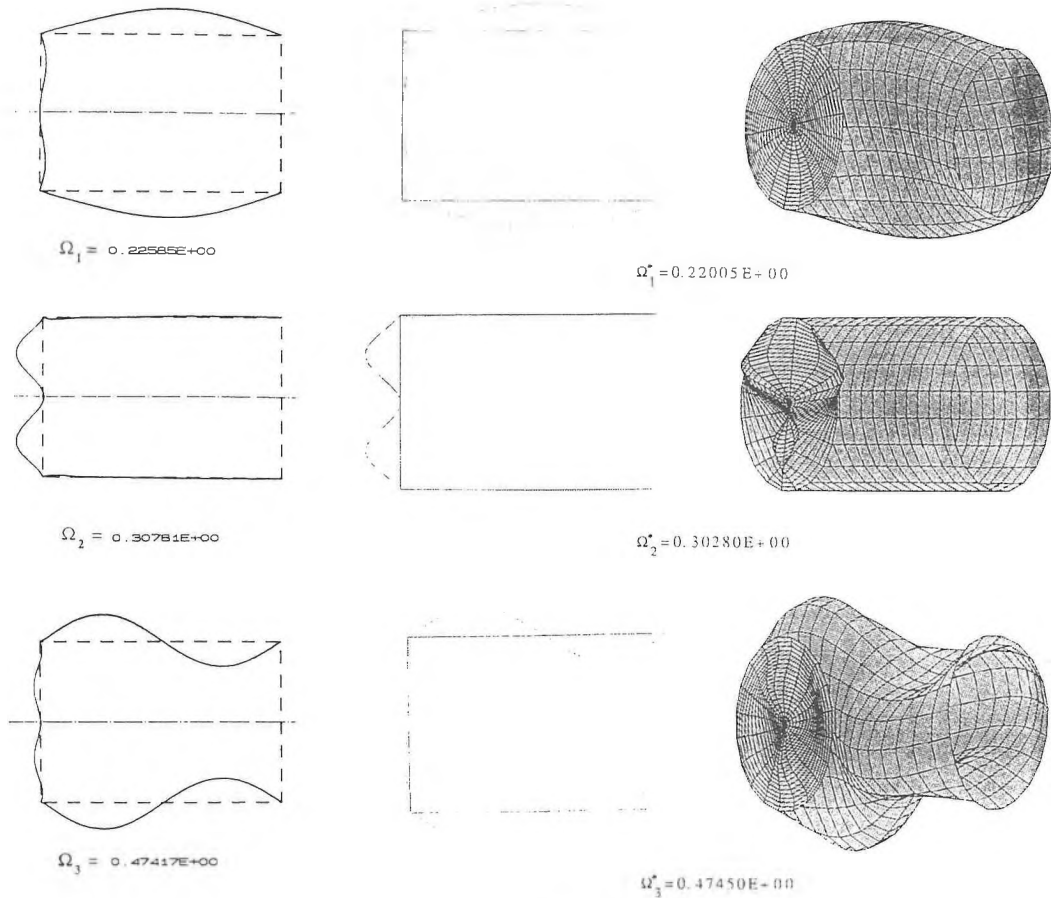


Fig.4. Comparison of the present approach with Finite element analysis in terms of mode shapes of the combined structure.

corresponding to the case in which the shell and plate displacements are of the same order of magnitude.

Concerning the second point mentioned above, it can be shown that a well-coupled mode occurs when there is a mechanical impedance match of the uncoupled structures, whereas panel-like or shell-like modes correspond to the case where the mechanical impedances of the uncoupled components are quite different.

4.2 Effect of bulkhead on the cabin noise

The information concerning the mechanical vibration of the structure is essential, but still not sufficient for noise control problems. Generally speaking, the understanding of vibrational phenomena is easier than that of the structural radiation, whereas without the latter, the structural quietening can hardly be achieved. In fact, the physical process by which the vibrating energy is converted to acoustical energy is rather complex. As a direct application of the established model, this section will concentrate on the cabin noise radiated by the end bulkhead. In order to simplify the discussion, the cylindrical shell is considered purely as an acoustically rigid wall, so that its vibration is not under consideration here. This analysis, neglecting obviously the effects of the cylinder, is the first step toward a more complete model. Particular effort is made to give a thorough understanding of the fixing conditions of this plate, which can hopefully help engineers to reduce the cabin noise. The model we have developed offers great advantages for investigating this problem, since different fixing conditions can be easily simulated by adjusting the elastic stiffness of the springs.

Numerical results are presented in the following order: First, a typical calculated vibration spectrum is presented and compared to experimental results. Then, two plates with two limiting fixing conditions are considered, illustrating the importance of certain parameters. It should be pointed out that one of the plates used in the discussion is a free plate. Although free supports can hardly be justified in practical circumstances for cavity configurations, this represents as a very informative reference case for understanding the phenomena. Meanwhile, as will be illustrated later, with decreasing support stiffness, the phenomena observed in the free case becomes rather representative of more realistic cases. Finally, calculations are made with a scaled down aircraft model. In this case, more realistic support cases are investigated.

Mechanical response of the plate

The study of the end plate which simulates the rear pressure bulkhead is of particular importance to our problem. One may hope to improve the internal sound field by modifying its designing. Fig.5 shows a comparison between our calculation and experimental measurement in terms of the average quadratic velocity of a plate. The plate is an

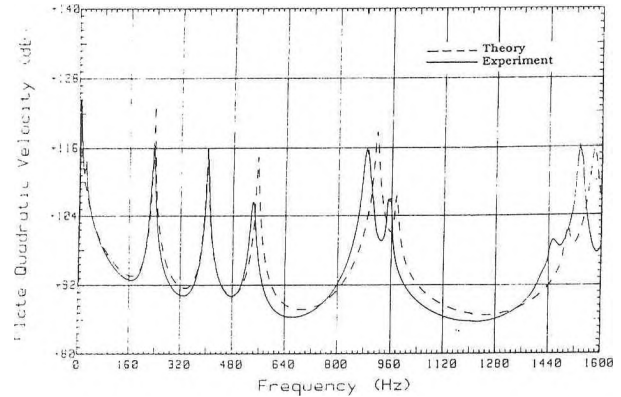


Fig.5. Comparison of the theory with experiment in terms of the plate's vibration

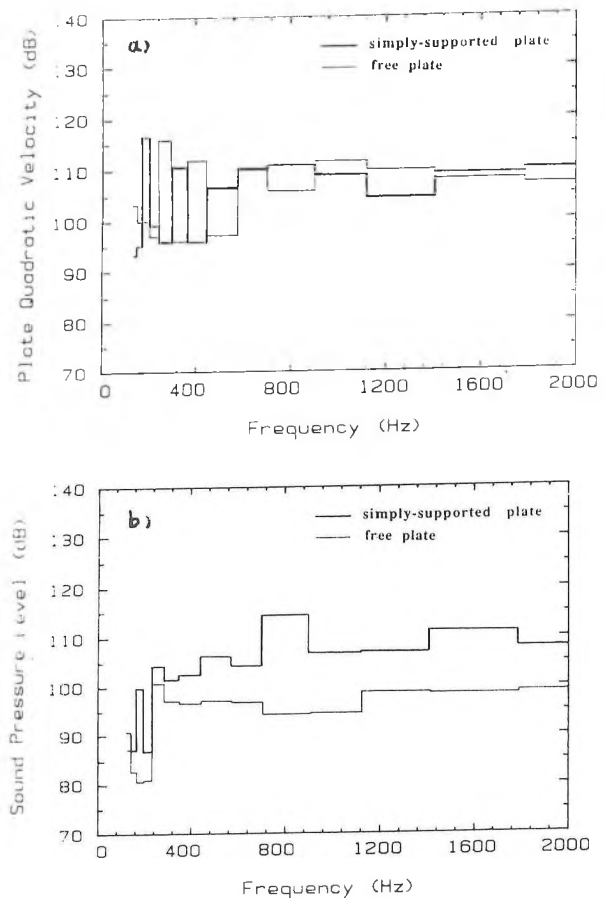


Fig.6. System response in one-third octave bands for plates with two limiting fixing conditions. a). average quadratic velocity of the plate. b). overall sound pressure level inside the cavity

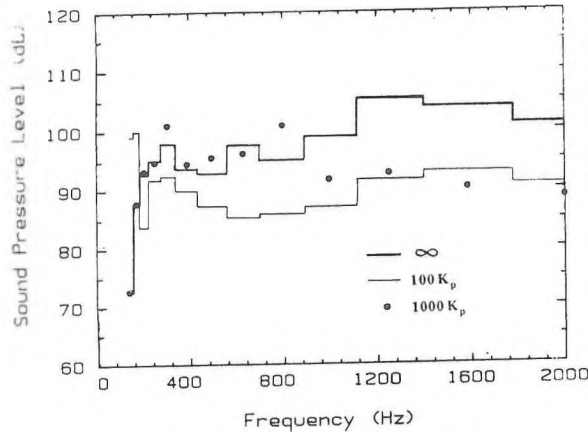


Fig. 7. Sound pressure level inside the cabin of a 1/4 scaled airplane model. Three fixing conditions of the RPB are considered

aluminium one of 0.132 m radius and 3.2 mm thickness. Although our model allows investigating plates with different boundary conditions, only a free plate, which is the most simple to realize experimentally, is chosen. To this end, the plate is suspended at three points along the boundary by elastical strings with small elastic constant. The comparison is made for a frequency range up to 1.6 kHz and good agreement exists between two sets of results. The differences in peak level comes from rough estimations of the structural damping. In fact, no damping measurement is made for the plate and the loss factor of the plate is set to be of 0.01 in the calculation.

Plates with two limiting fixings

The following configuration will be used for numerical investigations: it is a steel plate of 0.25m radius and 0.003 m thickness, backed by an air-contained cylindrical cavity of 0.6m thickness. The plate is driven by a unit point-force at $r_F = 0.1$ m and $\theta_F = 0$. The loss factors of the plate and the cavity are assumed to be constant: $\eta_v = \eta_p = 0.01$.

Fig.6(a-b) present the average quadratic velocity of the plates $\langle V^2 \rangle$ and the corresponding sound pressure level inside the cavity L_p for two limiting fixing cases: plates with simple supports and free supports. All spectra are presented in one-third octave band. $\langle V^2 \rangle$ is also given in dB with a reference of $2.5e-15$ (m^2/s^2). Fig.6a indicates that in terms of the quadratic velocity of the plate $\langle V^2 \rangle$, the overall level of the plate vibration is comparable. The difference can be shown to be caused basically by the different positions of the plate-controlled resonances. However, Fig.6b, comparing the corresponding average sound pressure level within the cavity clearly shows that the free plate radiates much less than a simply supported one. In fact, the sound pressure level induced by the free

plate is 10-20 dB lower than the one radiated by a simply-supported plate for almost the whole frequency range considered in the present case. Hence, it seems that the translational stiffness of the contour supports is a key factor in the radiation behavior of the plates into the cavity.

Plates with elastical supports (1/4 aircraft model)

Using this model, a prediction is made for a 1/4 scale model of the aircraft mentioned at the beginning of the paper. The cabin is faithfully scaled in every respects, Whereas the rear pressure bulkhead is simulated by a 3 mm thick plate. Fig.7 illustrates the cabin noise level in one-third octave band radiated by bulkheads with three different supports in translation. Three stiffnesses chosen are respectively infinite, $100K_p$ and $1000K_p$. Compared with the simply-supported plate case (with infinite stiffness), a limiting frequency seems to exist for each elastical support, above which we notice a significant reduction in induced sound pressure, but below which, a softer support does not always guarantee a sound reduction. The reason is that different supporting conditions modify the structural modes, the consequence of which can further change the modal structural-cavity coupling. As a result, in these frequency ranges, the cavity sound pressure may be amplified. Furthermore, the stiffer the support is, the higher is this limiting frequency and, consequently, the higher is the frequency range where the beneficial effect is expected. This phenomena has been found and analysed in detail in an other work [7]. In conclusion, a softer translational support of this bulkhead can improve significantly the cabin noise. In practical, the flexible mounting of the bulkhead should be designed by considering the axial pressure loading it withstands. Consequently, a compromise exists between the mechanical performance and the noise attenuation.

5. CONCLUDING REMARKS

We have presented an analytical model aiming to investigate the vibroacoustic behavior of an aircraft structure. Important phenomena have been revealed through numerical investigations. The originalities of the findings are summarized as follows:

1).The proposed approach offers a new way of addressing mechanically coupled structures. In fact, The idea of using dynamic distribution of springs offers a new possibility of handling structural complexities at substructure junctions and at boundaries.

2).This method offers an alternative to purely numerical methods such as FEM usually used to address this kind of problem. As has been shown by the comparisons with FEM, our method is physical, convenient, and efficient in terms of computation time. However, it should be mentioned that this method and FEM are complementary in

the sense that FEM is surely more capable of tackling complex structures. Consequently, an analysis with the present model may serve as a preliminary step to later finite element analyses.

3). It opens a new and promising door to the vibroacoustic study of the plate-ended shell structure in which the fluid loading is included.

4). Numerical study of the effect of the bulkhead fixing furnishes useful sound-proofing guidance.

Of course, the established model is still a preliminary one, in which many complicating elements of a real aircraft are not taken into account. In fact, the modeling process is rather useful in the initial stage of aircraft conceptualization, when major components and their coupling mechanisms are being defined. It may provide designers with the major trends of the vibroacoustic performance of their products and guide soundproofing measures. The framework established in this paper allows an extension to include further complexities such as stringers and frames. What is required in this case is to include the energy terms for these elements into the functional expression. This constitutes a major advantage of the method used. The improvement of the model in this direction is the current work of the authors.

REFERENCES

1. R. Vaicaitis, "Recent research on noise transmission into aircraft", *The Shock and Vib. Digest* 14(8),13-18,1982
2. J. S. Mixon and A. Powell, "Review of recent research on interior noise of propeller aircraft", *J. Aircraft* 22(11), 932-949,1985
3. M. J. Smith, "Aircraft noise", Cambridge Univ. Press, p359,1989
4. C. F. Chao et al. "Coupling of finite element acoustic absorption models", *J. Sound and Vib.* 66(4),605-613,1979
5. J. F. Unruh, "Prediction of aircraft propeller-induced, structure-born interior noise", *J. Aircraft*, 25(8), 758-764,1988
6. R. H. Lyon and G. Maidanik, "Statistical method in vibration analysis", *A.I.A.A. J.* 2(6),1015-1024, 1964
7. F. Fahy and G. White, "Statistical energy analysis and vibrational power flow", 3rd international congress on intensity techniques. Senlis, 1990
8. L. Cheng and J. Nicolas, "Free vibration analysis of a cylindrical shell-circular plate system with general coupling and various boundary conditions", to appear in *J. Sound and Vib.* 154(2), 1992
9. L. Cheng and J. Nicolas, "Radiation of sound into a cylindrical enclosure from point-driven end plate with general boundary conditions", to appear in *J. Acous. Soc. Am.* March 1992.
10. R. Vaicaitis, "Noise transmission into a light aircraft", *J. Aircraft* 17(2), 81-86,1980
11. L. R. Koval, "On sound transmission into a thin cylindrical shell under flight conditions", *J. Sound and Vib.* 48(2),265-275,1976
12. M. Barbeé *et al.*, "Transmission du son par des fuselage d'avion", 27ieme colloque d'aéronautique appliquée, Marseille, oct. 1990
13. A. Berry, J. L. Guyader and J. Nicolas, "A general formulation for the sound radiation from rectangular, baffled plates with arbitrary boundary conditions", *J. Acous. Soc. Am.* 88, 2792 - 2812, 1990
14. P. M. Morse and K. U. Ingard, "Theoretical acoustics", McGraw-Hill, New York,1968, Chap.9, pp.467-607

ACKNOWLEDGMENT

The Canadian Acoustical Association is greatly acknowledged for its awarding of the CAA Edgar and Millicent Shaw Postdoctoral Prize in Acoustics to the first author; it has in part supported the present research. This work was also supported by a grant from Canadair whose efficient collaboration is very much appreciated. We also acknowledge the assistance of J. Allard and E. Rébillard, who provided some of the results used in this paper. We also thank Murray Hodgson for doing the English revision of this paper.

MICROPHONES FROM LARSON-DAVIS LABORATORIES



- Preamplifiers
- Power Supplies
- Calibrators

PRECISE, RUGGED, AND AFFORDABLE

Individualized Calibration Charts

MICROPHONE CALIBRATION CHART

MODEL NO. _____

SERIAL NO. _____

SENSITIVITY @ 1013 mbar & 250 Hz

dB re 1V/Pascal

mV/Pascal

K_c (dB re 50 mV/Pascal)

CAPACITANCE @ 250 Hz

TEST CONDITIONS:

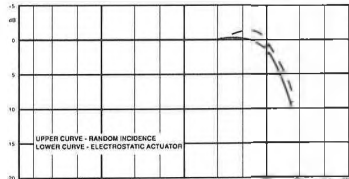
Polarization Voltage _____ V

Ambient Pressure _____ mbar

Temperature _____ °C

Relative Humidity _____ %

Date: _____ Signature: _____



Dalimar

Instruments Inc.

89, boul. Don Quichotte
Suite No. 7
Ile Perrot, Qc
J7V 6X2
Tel.: (514) 453-0033
Fax: (514) 453-0554



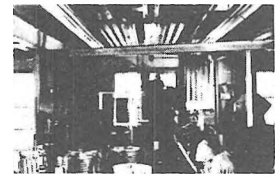
Noise Control Products & Systems

for the protection of personnel...
for the proper acoustic environment...

engineered to meet the requirements of Government regulations

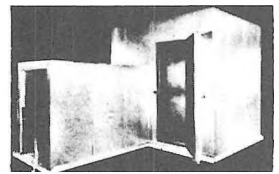
Eckoustic® Functional Panels

Durable, attractive panels having outstanding sound absorption properties. Easy to install. Require little maintenance. EFPs reduce background noise, reverberation, and speech interference; increase efficiency, production, and comfort. Effective sound control in factories, machine shops, computer rooms, laboratories, and wherever people gather to work, play, or relax.



Eckoustic® Enclosures

Modular panels are used to meet numerous acoustic requirements. Typical uses include: machinery enclosures, in-plant offices, partial acoustic enclosures, sound laboratories, production testing areas, environmental test rooms. Eckoustic panels with solid facings on both sides are suitable for constructing reverberation rooms for testing of sound power levels.



Eckoustic® Noise Barrier

● Noise Reduction Curtain Enclosures

The Eckoustic Noise Barrier provides a unique, efficient method for controlling occupational noise. This Eckoustic sound absorbing-sound attenuating material combination provides excellent noise reduction. The material can be readily mounted on any fixed or movable framework of metal or wood, and used as either a stationary or mobile noise control curtain.

● Machinery & Equipment Noise Dampening

**Acoustic Materials
& Products for
dampening and reducing
equipment noise**

Multi-Purpose Rooms

Rugged, soundproof enclosures that can be conveniently moved by fork-lift to any area in an industrial or commercial facility. Factory assembled with ventilation and lighting systems. Ideal where a quiet "haven" is desired in a noisy environment: foreman and supervisory offices, Q.C. and product test area, control rooms, construction offices, guard and gate houses, etc.



Audiometric Rooms: Survey Booths & Diagnostic Rooms

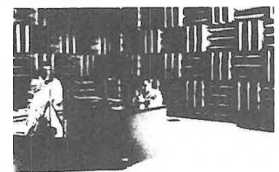
Eckoustic Audiometric Survey Booths provide proper environment for on-the-spot basic hearing testing. Economical. Portable, with unitized construction.

Diagnostic Rooms offer effective noise reduction for all areas of testing. Designed to meet, within ± 3 dB, the requirements of MIL Spec C-81016 (Weps). Nine standard models. Also custom designed facilities.



An-Eck-Oic® Chambers

Echo-free enclosures for acoustic testing and research. Dependable, economical, high performance operation. Both full-size rooms and portable models. Cutoff frequencies up to 300 Hz. Uses include: sound testing of mechanical and electrical machinery, communications equipment, aircraft and automotive equipment, and business machines; noise studies of small electronic equipment, etc.



For more information, contact

ECKEL INDUSTRIES OF CANADA, LTD., Allison Ave., Morrisburg, Ontario • 613-543-2967

ECKEL INDUSTRIES, INC.